SPATIAL STRUCTURES OF ENERGY TRANSFERS IN ELASTIC WAVE TURBULENCE

Masanori Takaoka[1] & Naoto Yokoyama [2]
[1]*Department of Mechanical Engineering, Doshisha University, Kyotanabe, Japan*
[2]*Department of Aeronautics and Astronautics, Kyoto University, Kyoto, Japan*

Abstract Spatial structures of energy transfers in both the real and Fourier spaces are investigated by simulating the Föppl-von Kármán (FvK) equation. Distinctive structures of the stretching-energy field, which is the bundle of ridges in the real space and the line segment at small wavenumbers in the Fourier space, appear in the active phases of turbulent state.

INTRODUCTION AND FORMULATION

Elastic wave turbulence has been studied experimentally, numerically and theoretically, and exhibited rich phenomena such as spectral variation [1]. The coexistence of weakly and strongly nonlinear spectra is one of the most remarkable properties. In [2], energy decomposition analysis and energy budget are investigated by using a single-wavenumber representation of nonlinear energy spectrum. We also have found the strong correlation between a mode $a_{\boldsymbol{k}}$ and its companion mode $a_{-\boldsymbol{k}}$ at the small wavenumbers $\boldsymbol{k}$, where the nonlinearity is relatively strong. Although one may expect a distinctive structure in the real space due to this correlation, the real-space structures are the results from the cumulative effect of all active modes. At the 3rd IC-MSQUARE 2014 [3], on the other hand, we have reported that the bundle structures of ridges appear intermittently in the time evolution of the stretching-energy field. The time evolution of nonlinearity shows the existence of active and moderate phases in the turbulent state. The bundle structures appear at such active phases with the strong nonlinearity, when the energy transfers occur effectively at the scales of strongly nonlinear spectrum. We attempt to characterize this driving structure of energy transfer in both the real and Fourier spaces.
The governing equation for the lateral displacement ζ and the momentum p in a thin elastic plate is the FvK equation,

$$\frac{\partial p}{\partial t} = -\frac{Yh^2}{12(1-\sigma^2)}\Delta^2\zeta + \{\zeta,\chi\}\,, \quad \frac{\partial \zeta}{\partial t} = \frac{p}{\rho}, \quad \Delta^2\chi = -\frac{Y}{2}\{\zeta,\zeta\}\,, \tag{1}$$

where χ is the Airy stress potential. The Laplace operator and the Monge–Ampère operator are expressed as Δ and $\{f,g\} = \partial_{xx}f\partial_{yy}g + \partial_{yy}f\partial_{xx}g - 2\partial_{xy}f\partial_{xy}g$, respectively. The Young's modulus Y, the Poisson ratio σ, and the density ρ are the physical properties of the plate. The thickness of the plate is expressed by h. The complex amplitude $a_{\boldsymbol{k}}$ is used as the elementary wave of the wavenumber $\boldsymbol{k}$ in weak turbulence theory (WTT). The Fourier coefficients of the displacement $\zeta_{\boldsymbol{k}}$, of the momentum $p_{\boldsymbol{k}}$, and of the Airy stress potential $\chi_{\boldsymbol{k}}$, respectively are given as

$$\zeta_{\boldsymbol{k}} = \frac{a_{\boldsymbol{k}} + a^*_{-\boldsymbol{k}}}{\sqrt{2\rho\omega_{\boldsymbol{k}}}}, \quad p_{\boldsymbol{k}} = -i\sqrt{\frac{\rho\omega_{\boldsymbol{k}}}{2}}(a_{\boldsymbol{k}} - a^*_{-\boldsymbol{k}}), \quad \chi_{\boldsymbol{k}} = -\frac{Y}{4\rho k^4}\sum_{\boldsymbol{k}_1+\boldsymbol{k}_2=\boldsymbol{k}}\frac{|\boldsymbol{k}_1\times\boldsymbol{k}_2|^2}{\sqrt{\omega_{\boldsymbol{k}_1}\omega_{\boldsymbol{k}_2}}}(a_{\boldsymbol{k}_1} + a^*_{-\boldsymbol{k}_1})(a_{\boldsymbol{k}_2} + a^*_{-\boldsymbol{k}_2}), \tag{2}$$

where $\omega_{\boldsymbol{k}} = \sqrt{Yh^2/12(1-\sigma)^2\rho}\,k^2$, and a^* represents the complex conjugate of a. Equation (1) is reduced to a single equation for $a_{\boldsymbol{k}}$, which was solved numerically by using the standard pseudo-spectral method.
The energy decomposition is convenient to investigate the energy budget in detail. [2] The decomposed energies are the kinetic energy K, the bending energy $V_{\rm b}$ and the stretching energy $V_{\rm s}$:

$$K(\boldsymbol{x}) = \frac{p^2}{2\rho}, \quad V_{\rm b}(\boldsymbol{x}) = \frac{Yh^2\left((\Delta\zeta)^2 - (1-\sigma)\{\zeta,\zeta\}\right)}{24(1-\sigma^2)}, \quad V_{\rm s}(\boldsymbol{x}) = \frac{(\Delta\chi)^2 - (1+\sigma)\{\chi,\chi\}}{2Y}. \tag{3}$$

Adoption of $\zeta_{\boldsymbol{k}}$, $p_{\boldsymbol{k}}$ and $\chi_{\boldsymbol{k}}$ as elementary waves enable the single-wavenumber representations of these decomposed energies under the periodic boundary condition: $K_{\boldsymbol{k}} = |p_{\boldsymbol{k}}|^2/2\rho$, $V_{{\rm b}\boldsymbol{k}} = \rho\omega_{\boldsymbol{k}}^2|\zeta_{\boldsymbol{k}}|^2/2$, $V_{{\rm s}\boldsymbol{k}} = k^4|\chi_{\boldsymbol{k}}|^2/2Y$. We here categorize the former two energies (latter one energy) linear (nonlinear) energy, since their (its) order of the complex amplitudes is quadratic (quartic). It may be worth to note here that adoption of the complex amplitudes as elementary waves makes the nonlinear energy, $V_{{\rm s}\boldsymbol{k}}$, the convolution representation as known in WTT.

RESULTS AND CONCLUSION

Time evolution of nonlinearity, which is estimated by the ratio of the quartic to quadratic order of the complex amplitude in Hamiltonian, shows the existence of active and moderate phases in the turbulent state, as shown in Fig. 1 (a). The strong nonlinearity appears intermittently, while the nonlinearity fluctuates randomly with relatively small amplitudes mostly. To find the typical structures of nonlinearity in the real space, we have drawn several kinds of fields, such as $\zeta(\boldsymbol{x})$, $p(\boldsymbol{x})$, $K(\boldsymbol{x})$, $V_{\rm b}(\boldsymbol{x})$, and $V_{\rm s}(\boldsymbol{x})$. The field $\zeta(\boldsymbol{x})$ has relatively large-scale structures, while the other fields have very

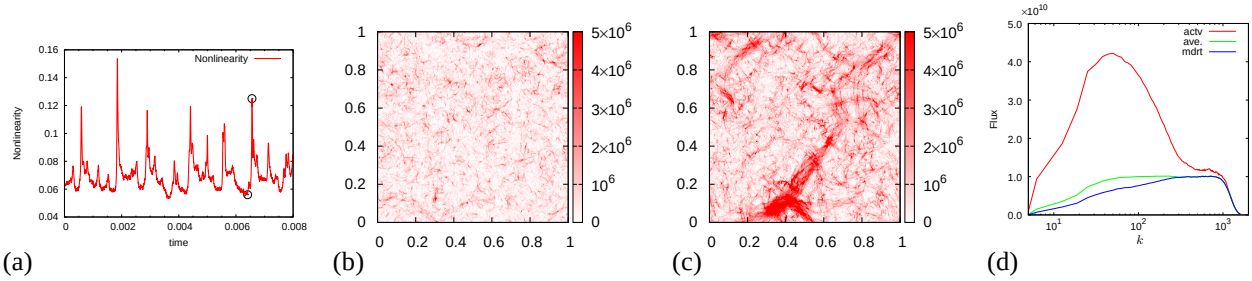

Figure 1. (a) Time evolution of nonlinearity. Representative snapshot of $V_{\rm s}(\boldsymbol{x})$ in (b) moderate and (c) active phases. (d) Representative energy fluxes in active (red) and moderate (blue) phases and their average (green).

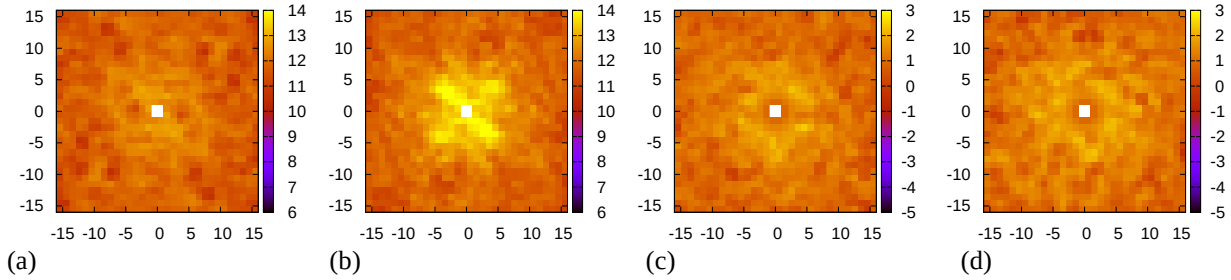

Figure 2. Snapshot of the logarithmic amplitude scales of $k^2\chi_{\boldsymbol{k}}$ in (a) moderate and (b) active phases. Snapshot of the logarithmic amplitude scales of $a_{\boldsymbol{k}}$ in (c) moderate and (d) active phases. The scale markings of the axes are expressed in 2π unit.

fine non-uniform distribution that consists of point-like structures. Only the stretching-energy field $V_{\rm s}(\boldsymbol{x})$ shows the clear difference of structures between active and moderate phases.

In Figs. 1 (b) and (c) shown are the snapshots of $V_{\rm s}(\boldsymbol{x})$ at moderate and active phases in the turbulent state, respectively. The bundle structures of the ridges of stretching energy are observed in the latter figure. We also examined the fluxes of the total energy in each phases, since they reflect the nonlinear interaction among modes. Note that the fluxes are different from those of linear energy conventionally used in WTT. Although the averaged energy flux, green curve in Fig. 1 (d), is almost constant in the inertial range, each representative flux deviates from the average value significantly (slightly) in low (high) wavenumber region where the strongly (weakly) nonlinear spectrum is observed. The results Figs. 1 suggest the bundle structures found in the real space drive energy transfer.

Figures. 2 (a) and (b) respectively show the corresponding snapshot of $k^2\chi_{\boldsymbol{k}}$ in the Fourier space. We can clearly see the X-structure of $k^2\chi_{\boldsymbol{k}}$, whose direction is perpendicular to that of the real-space structures, at small wavenumbers in the latter figure, which is the natural consequence of the duality between the real and Fourier spaces. Since we can reproduce the bundle structures by retaining only the mode within the range $k = \sqrt{k_x^2 + k_y^2} \leq 5 \times 2\pi$, the nonlinear interaction among the modes might be conducted by these small number of modes. Since $\chi_{\boldsymbol{k}}$ consists of $a_{\boldsymbol{k}}$, one may expect the difference of structures in $a_{\boldsymbol{k}}$ between active and moderate phases in the turbulent state. Figures. 2 (c) and (d) respectively show the corresponding snapshot of $a_{\boldsymbol{k}}$ in the Fourier space. It should be noted here that $a_{\boldsymbol{k}}$ is not the Hermitian function of $\boldsymbol{k}$ in contrast with $\zeta_{\boldsymbol{k}}$, $p_{\boldsymbol{k}}$, and $\chi_{\boldsymbol{k}}$. Little difference can be seen there. We also examined $\zeta_{\boldsymbol{k}}$ and $p_{\boldsymbol{k}}$, though the graphs are omitted here. No clear structures can be seen there. While little difference appears in $a_{\boldsymbol{k}}$ as well as $\zeta_{\boldsymbol{k}}$ and $p_{\boldsymbol{k}}$, clear difference appears $\chi_{\boldsymbol{k}}$ which is a kind of the convolution of $a_{\boldsymbol{k}}$.

In [4], we report the importance of $\chi_{\boldsymbol{k}}$ at small wavenumbers in the nonlocal interactions of the kinetic-energy transfer. It means that the bundle structure observed in the real space homologizes this interaction among the Fourier modes [3]. The mechanism how the functional form of $\chi_{\boldsymbol{k}}$ extracts the nonlinear effects from the complex amplitude $a_{\boldsymbol{k}}$ will be discussed.

References

[1] N. Yokoyama and M. Takaoka. Weak and strong wave turbulence spectra for elastic thin plate. *Phys. Rev. E* **89**: 012909, 2014.
B. Miquel and N. Mordant. Nonstationary wave turbulence in an elastic plate. *Phys. Rev. Lett.* **107**: 034501, 2011.

[2] N. Yokoyama and M. Takaoka. Single-wave number representation of nonlinear energy spectrum in elastic-wave turbulence of the Föppl-von Kármán equation: Energy decomposition analysis and energy budget. *Phys. Rev. E* **90**: 063004, 2014.

[3] M. Takaoka and N.Yokoyama. Bundle structures of stretching-energy and nonlinear interactions among modes in elastic wave turbulence. *J. Phys.: Conf. Ser.* **574**: 012030, 2015.

[4] N. Yokoyama and M. Takaoka. A numerical analysis of detailed energy transfers in elastic-wave turbulence. *ETC 15*